

MEASUREMENT OF THE NEUTRAL TO CHARGED CURRENT
CROSS SECTION RATIO IN NEUTRINO AND ANTINEUTRINO INTERACTIONS

M. Holder, J. Knobloch, J. May, H.P. Paar, P. Palazzi, F. Ranjard,
D. Schlatter, J. Steinberger, H. Suter, H. Wahl, S. Whitaker
and E.G.H. Williams
CERN, Geneva, Switzerland

F. Eisele, C. Geweniger, K. Kleinknecht, G. Spahn and H-J. Willutzki
Institut für Physik^{*)} der Universität, Dortmund, Germany

W. Dorth, F. Dydak, V. Hepp, K. Tittel and J. Wotschack
Institut für Hochenergiephysik^{*)} der Universität, Heidelberg, Germany

A. Berthelot, P. Bloch, B. Devaux, M. Grimm, J. Maillard,
B. Peyaud, J. Rander, A. Savoy-Navarro and R. Turley
D.Ph.P.E., CEN-Saclay, France

F.L. Navarra
Istituto di Fisica dell'Università, Bologna, Italy

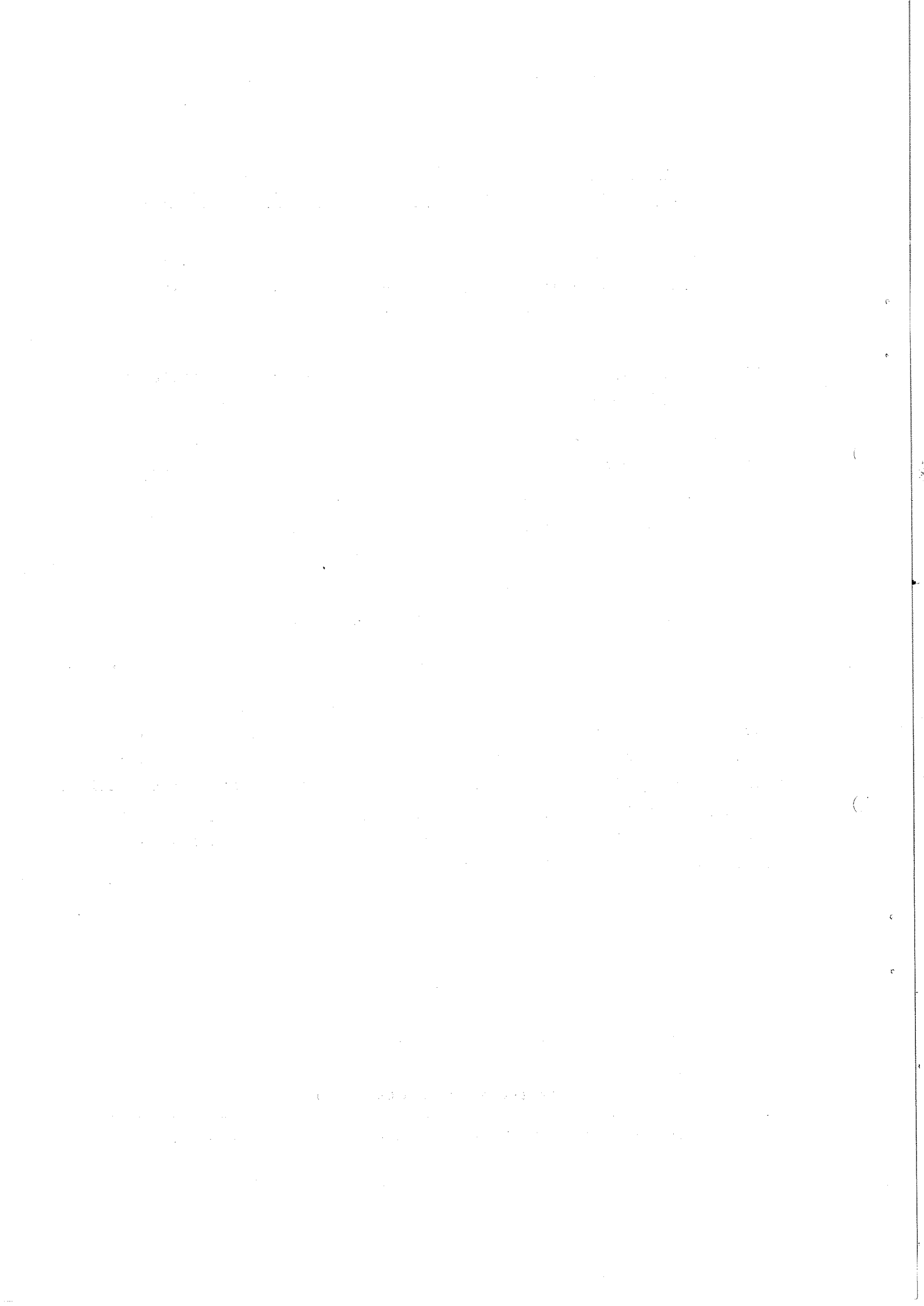
ABSTRACT

We report on the analysis of inclusive neutral current events produced in neutrino and antineutrino narrow band beams. We find for incident neutrino energies in the range 12 - 200 GeV and for hadron energies above 12 GeV a neutral to charged current cross-section ratio of $R_{\nu} = 0.293 \pm 0.010$ for incident neutrinos, and $R_{\bar{\nu}} = 0.35 \pm 0.03$ for antineutrinos. These ratios are consistent with the Weinberg-Salam model, with $\sin^2\theta_w = 0.24 \pm 0.02$.

Geneva - 15 August 1977

(Physics Letters B)

*) Supported by Bundesministerium für Forschung und Technologie



Since the discovery of the semi-leptonic neutral current interaction, $\nu(\bar{\nu}) + N \rightarrow \nu(\bar{\nu}) + \text{hadrons}^1)$, interest has been concentrated on precise measurements of its strength and structure. We have measured inclusive neutral current (NC) interactions on iron nuclei induced by neutrinos and antineutrinos. In this letter we present results on the ratios of neutral to charged current (CC) inclusive cross-sections for neutrinos (R_{ν}) and antineutrinos ($R_{\bar{\nu}}$).

The experiment has been performed in the narrow-band neutrino beam at the CERN SPS. The incident neutrinos are produced by the decay of charge selected pions and kaons in a parallel beam of well defined momentum, 200 ± 9 (rms) GeV/c. Figure 1 shows the primary energy spectrum for neutrinos (Fig. 1a) and antineutrinos (Fig. 1b).

The detector²⁾ combines the function of target, hadron calorimeter, and muon spectrometer integrally in 19 similar modules. Each module consists of multiple iron plates 3.75 m in diameter, with a total thickness of 75 cm of iron and a weight of 65 tons per module. The hadron shower is measured by means of scintillator sheets divided into eight horizontal strips inserted between the iron plates. The first seven modules are equipped with scintillators placed every 5 cm of iron, the next eight sample every 15 cm, and the last four every 75 cm. The vertical position of the showers is determined by weighting coordinates of the scintillator strips with their energy response. The horizontal shower position is calculated from the ratio of the pulseheights at the right and left scintillator edge, making use of the light absorption in the scintillator sheets (absorption length ~ 2 m). The radial distance R of each event is thus determined with a resolution of $\sigma = 22$ cm. The trigger relevant to this analysis requires an energy deposition of more than 3 GeV in the detector.

Events with a hadron-shower of at least 12 GeV are selected; this is well above the hardware trigger threshold. The vertex position z_V along the beam direction is chosen in the interval $35 < z_V < 825$ cm of iron. The lower cut excludes possible neutron induced showers in the front part of the spectrometer although we have no evidence for such an effect. The upper cut allows for a sufficient penetration depth in the rear part of the spectrometer to be used for the separation of NC and CC events. The overall length of iron is 1425 cm.

To minimize problems of side leakage, the radial distance R is required to be less than 1.6 m.

For each event, an event length L is calculated from the scintillator information and is equal to the thickness of iron between the vertex and the end of the event, measured parallel to the axis of the detector. In Fig. 2 the distribution of L is shown for neutrinos (Fig. 2a) and antineutrinos (Fig. 2b). We see a strong signal of NC events for an event length less than 200 cm of iron. The region above 200 cm is rather flat and consists of CC events with a short muon track. It is emphasized that in our analysis no muon reconstruction is required. Also, by virtue of the large diameter of our set-up, the background of CC events in the NC signal is mostly due to stopping muons rather than due to muons escaping at the side.

A NC candidate is defined by the requirement: $16 < L < L_{\text{cut}}$ (cm of iron), where L_{cut} is made logarithmically dependent on the hadron energy. The parametrization is $L_{\text{cut}} = 75 + 38 \times \ln E_{\text{H}}$ (cm of iron), with E_{H} in GeV. The lower cut at 16 cm excludes most of the cosmic ray background. The NC event losses due to the lower and upper cuts in L are together of the order of 1%.

The CC background in the NC signal is determined on the basis of the observed events in a CC monitor region, defined by $311 < L < 511$ cm of iron.

To obtain the number of genuine NC and CC events, the following corrections to the number of candidates must be applied (see also Table 1):

1. Cosmic ray background: It is determined from the event rate out of time with the 23 μsec long beam spill. The difference of the electronics dead-time for events inside and outside the spill is accounted for. The contamination by cosmic ray muons is significant only for hadron energies below 15 GeV and is determined with good statistical and systematic accuracy.
2. Wide-band beam (WBB) background: In the region between the proton target and the beginning of the beam-forming elements, hadrons of both signs and with the full energy spectrum are present. Their decays give rise to a flux of both neutrinos and

antineutrinos. A subtraction of the events induced by the WBB flux is necessary because of the very different energy spectrum, peaking at low energies. It is determined in special runs where the momentum-defining collimator, located halfway downstream between the beam-forming elements, was closed. Thus the hadrons which normally produce the neutrinos are stopped there. The main flux of the WBB background does not point to our detector, however this sort of background constitutes a major source of statistical and systematic error in our analysis. A fraction of approximately 5% of the running time has been devoted to closed collimator studies. The events observed in these runs are scaled by the ratio of the collimator open and collimator closed fluxes. They are globally subtracted in the NC signal, CC signal and CC monitor region, respectively. The subtraction is of the order of 3% for neutrinos, and 20% for antineutrinos.

3. CC background: The CC events with an event length $L < L_{\text{cut}}$ must be subtracted from the NC candidates, and added to the CC candidates. Their number is determined by a Monte Carlo extrapolation from the measured number of events in the CC monitor region. For this extrapolation the distribution of the scaling variable $y = E_H/E_\nu$ is assumed to be $1 + \alpha_{\text{CC}}(1-y)^2$ for CC neutrino events, and $\alpha_{\text{CC}} + (1-y)^2$ for CC antineutrino events. In the quark parton model $\alpha_{\text{CC}} = \bar{q}/q$ measures the contribution of anti-quarks. We have chosen $\alpha_{\text{CC}} = 0.1$ independent of the neutrino energy³). However, since essentially only CC events with y near 1 constitute the background in the NC signal, this extrapolation is insensitive to the actual value of α_{CC} . The small contribution of events where the interaction takes place near the edge of the detector and the muon escapes, is taken into account by the Monte Carlo simulation. The systematic uncertainties in the extrapolation are estimated to be ~5% for neutrinos and ~8% for antineutrinos.
4. K_{e_3} background: Electron neutrinos produce CC and NC interactions in the detector, and all of them simulate NC interactions, because the electromagnetic cascade generated by the final state electron is contained in the hadron shower. The observed NC/CC ratio is therefore affected. The K_{e_3} decay is the only important source of

electron neutrinos. This background is suppressed by the relative branching ratio of the K_{e_3} and K_{μ_2} decays, and by the lower energy of the neutrinos produced in three body decays. The background is further reduced by the admixture of neutrinos arising from pion decay. Since the relative amount of kaons and pions in the parent beam is measured to be $K^+/\pi^+ = 0.17$ and $K^-/\pi^- = 0.05$, the K_{e_3} correction is straightforward. It amounts to ~10% for neutrinos and ~5% for antineutrinos, respectively.

In Table 1 the data reduction and the results on R_ν and $R_{\bar{\nu}}$ are summarized. With the exception of the final result, the quoted errors are statistical only. The quoted systematic error arises from the uncertainties in the CC background subtraction, the WBB background subtraction, and the K_{e_3} correction.

The final result for the ratio of the inclusive neutral to charged current cross sections on iron nuclei is:

$$\left. \begin{aligned} R_\nu &= (NC/CC)_\nu = 0.293 \pm 0.010 \\ R_{\bar{\nu}} &= (NC/CC)_{\bar{\nu}} = 0.35 \pm 0.03 \end{aligned} \right\} E_H > 12 \text{ GeV}$$

The average incident neutrino energy is 110 GeV for neutrinos, and 90 GeV for antineutrinos.

Our result is in agreement with the recent results of other experiments⁴⁻⁶), as shown in Fig. 3. However, when making a direct comparison of the measured ratios it should be kept in mind that the hadron energy cut-offs and the neutrino energy spectra are quite different. In particular, the cut-off correction is large for the Gargamelle values⁴). Since the cut-off correction is small for the high energy experiments, we prefer to compare our result, obtained with a cut-off, to the uncorrected values of the two other high-energy experiments^{5,6}), and to the corrected value of the low energy Gargamelle experiment⁴).

Our results may be compared with the prediction of the Weinberg-Salam model. For this purpose, the 12 GeV cut in the hadron energy, the small deviation of iron from an isoscalar target, and an assumed antiquark contribution of \bar{q}/q of 0.1 have been incorporated into the model (see also Fig. 3). The Weinberg mixing angle can be determined from R_ν and $R_{\bar{\nu}}$ separately, with the results:

From R_{ν} : $\sin^2\theta_w = 0.243 \pm 0.021$

From $R_{\bar{\nu}}$: $\sin^2\theta_w = 0.21 \pm 0.09$.

The quoted error includes variations of \bar{q}/q in the range $0.05 < \bar{q}/q < 0.20$. Both values are in good agreement, thus supporting the Weinberg-Salam model. Combining both results, we get

From R_{ν} and $R_{\bar{\nu}}$: $\sin^2\theta_w = 0.24 \pm 0.02$

We thank most sincerely our many technical collaborators and the members of the SPS staff for the operation of the accelerator.

REFERENCES

1. F.J. Hasert et al., Phys. Lett. 46B (1973) 121; 46B (1973) 138.
2. M. Holder et al., A detector for high-energy neutrino interactions, submitted to Nuclear Instrum. Methods.
3. M. Holder et al., Is there a high-y anomaly in antineutrino interactions? submitted to Phys. Rev. Lett.
4. J. Blietschau et al., Nucl. Phys. B118 (1977) 218.
5. B.C. Barish et al., Proc. Int. Neutrino Conf. Aachen, 1976 (F. Vieweg & Sohn, Verlagsgesellschaft mbH, Braunschweig, 1977), p. 289.
6. T.Y. Ling, Proc. Int. Neutrino Conf. Aachen, 1976 (F. Vieweg & Sohn, Verlagsgesellschaft mbH, Braunschweig, 1977), p. 296;
P. Wanderer et al., Measurement of the neutral current interactions, preprint HWPF-77/1, submitted to Phys. Rev. D.

	Neutrinos	Antineutrinos
NC candidates	10770 ± 104	3314 ± 58
Cosmic-ray background	-59 ± 7	-119 ± 10
WBB background	-286 ± 126	-646 ± 116
CC background	-1493 ± 64	-235 ± 49
NC with $L < 16$ and $L > L_{\text{cut}}$	+150	+43
K_{e3} correction	-1008	-154
NC signal	8074 ± 156	2203 ± 130
CC candidates	26509 ± 163	6483 ± 81
WBB background	-239 ± 117	-323 ± 83
CC extrapolation	+1467 ± 64	+253 ± 42
NC with $L > L_{\text{cut}}$	-134	-35
CC signal	27603 ± 211	6378 ± 123
NC/CC (error only statistical)	0.293 ± 0.006	0.346 ± 0.021
NC/CC (final result, systematic error included)	<u>0.293 ± 0.010</u>	<u>0.35 ± 0.03</u>

TABLE I

Data reduction for the ratio of neutral to charged current
inclusive cross-sections for $E_H > 12$ GeV

FIGURE CAPTIONS

- Fig. 1 : Monte Carlo simulation of the incident neutrino energy spectrum for neutrinos (a) and antineutrinos (b), with a cut in the radial distance $R < 1.6$ m.
- Fig. 2 : Event length distribution for neutrinos (a) and antineutrinos (b).
- Fig. 3 : Comparison of R_{ν} and $R_{\bar{\nu}}$ with the Weinberg-Salam model. In the model calculation, the cut $E_H > 12$ GeV, the neutron to proton ratio of iron, and an antiquark contribution of $\bar{q}/q = 0.1$ (solid line) and, for comparison, of $\bar{q}/q = 0$ (dashed line) are incorporated.

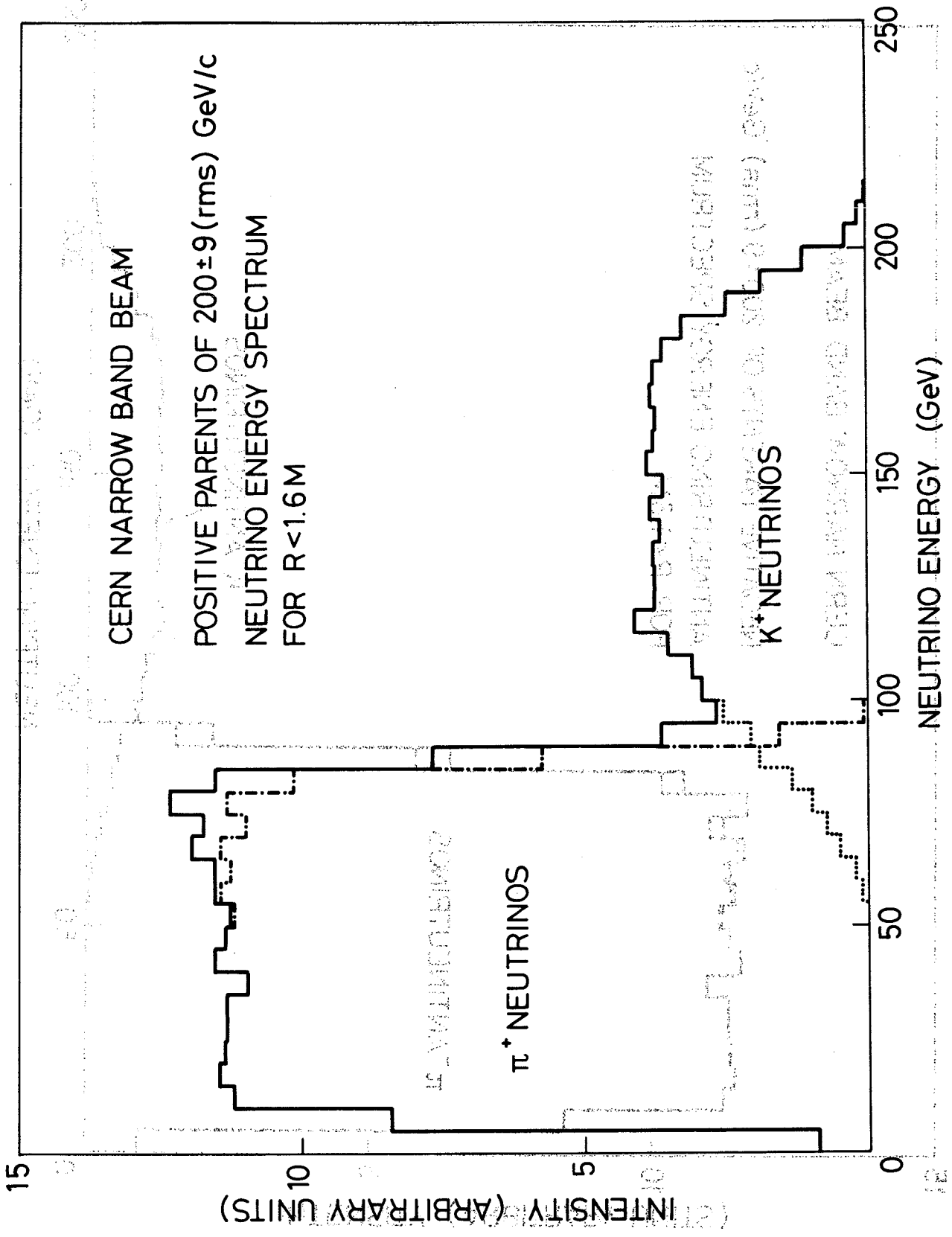


FIG. 1a

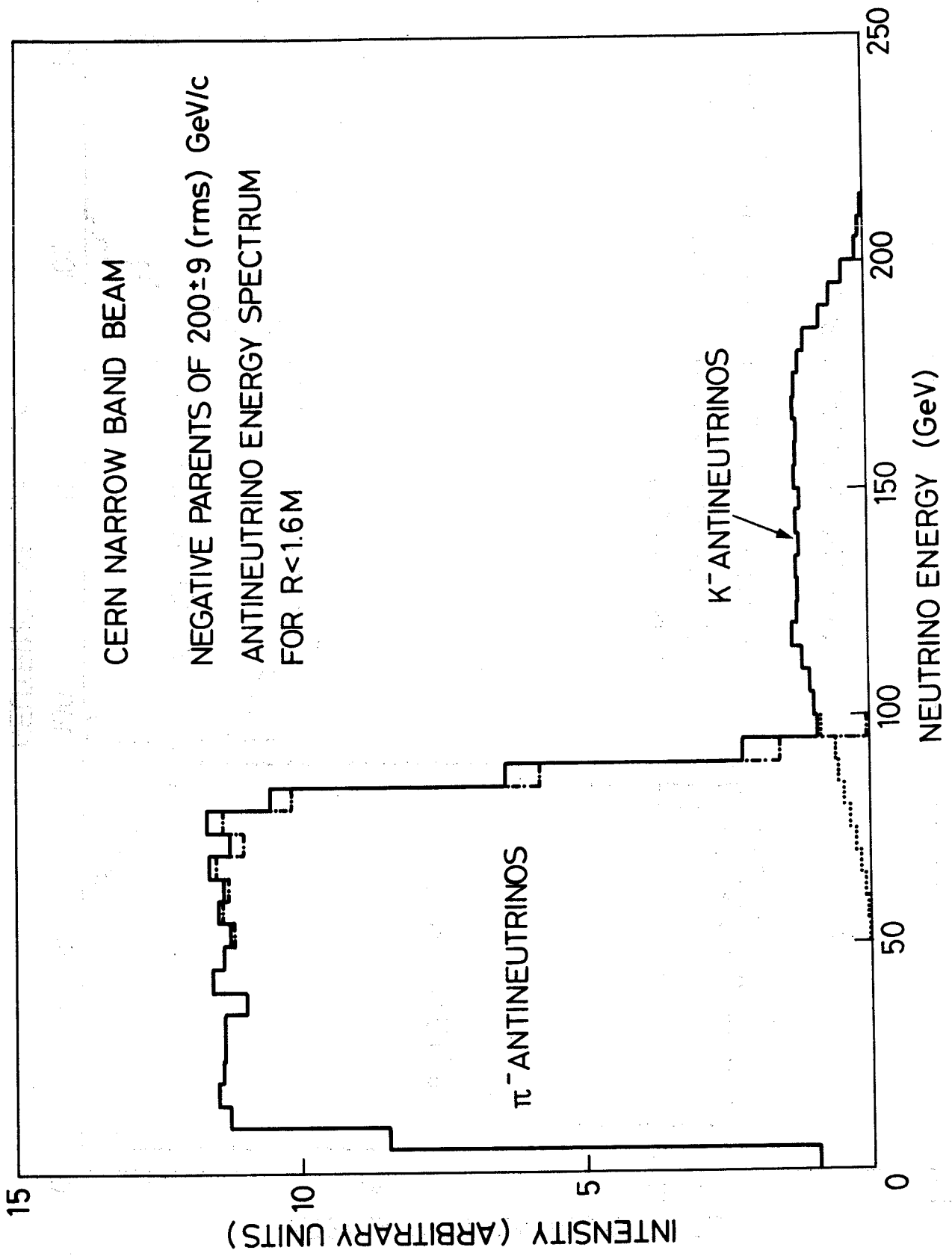


FIG. 1b

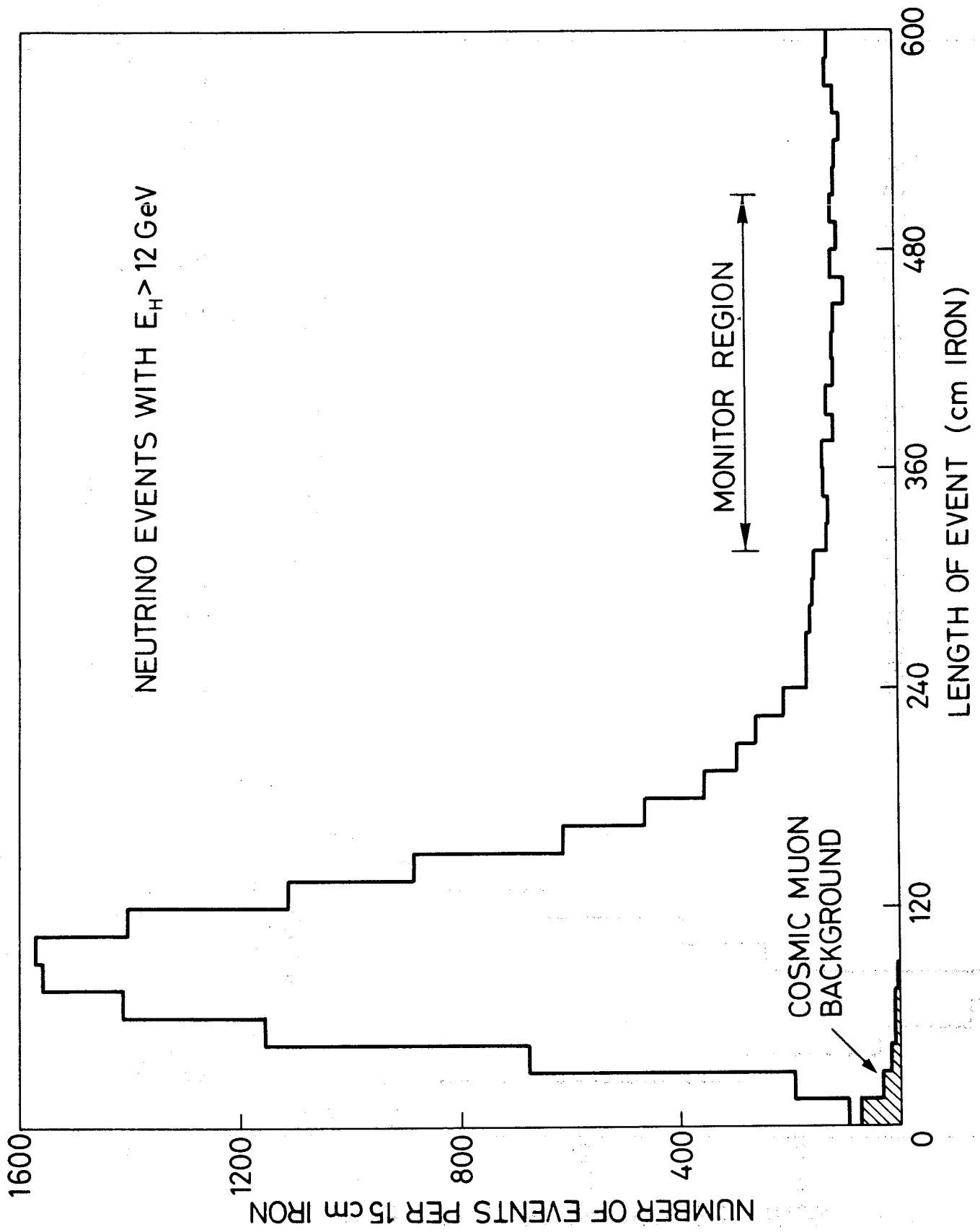


FIG. 2a

ANTINEUTRINO EVENTS WITH $E_H > 12 \text{ GeV}$

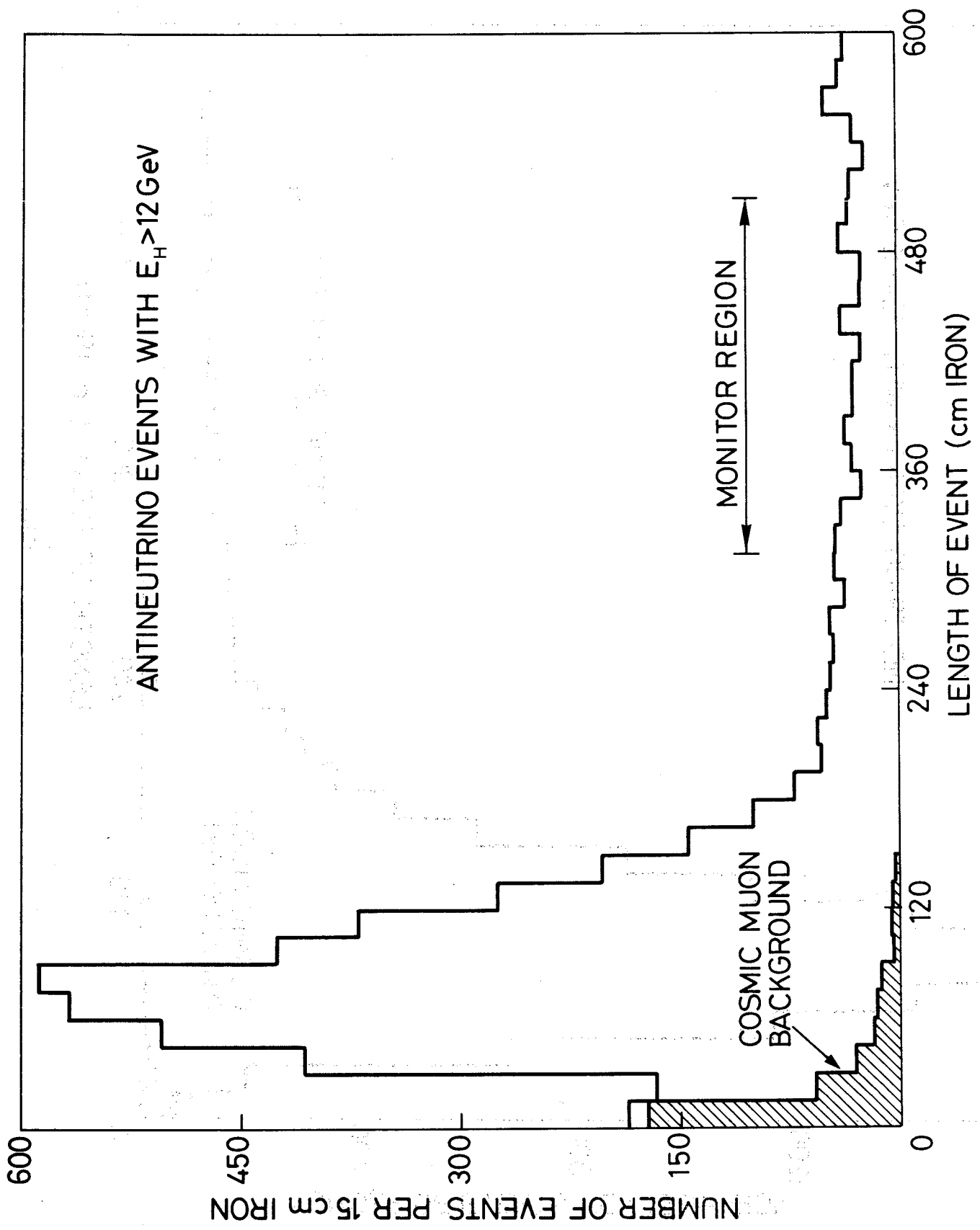


FIG. 2b

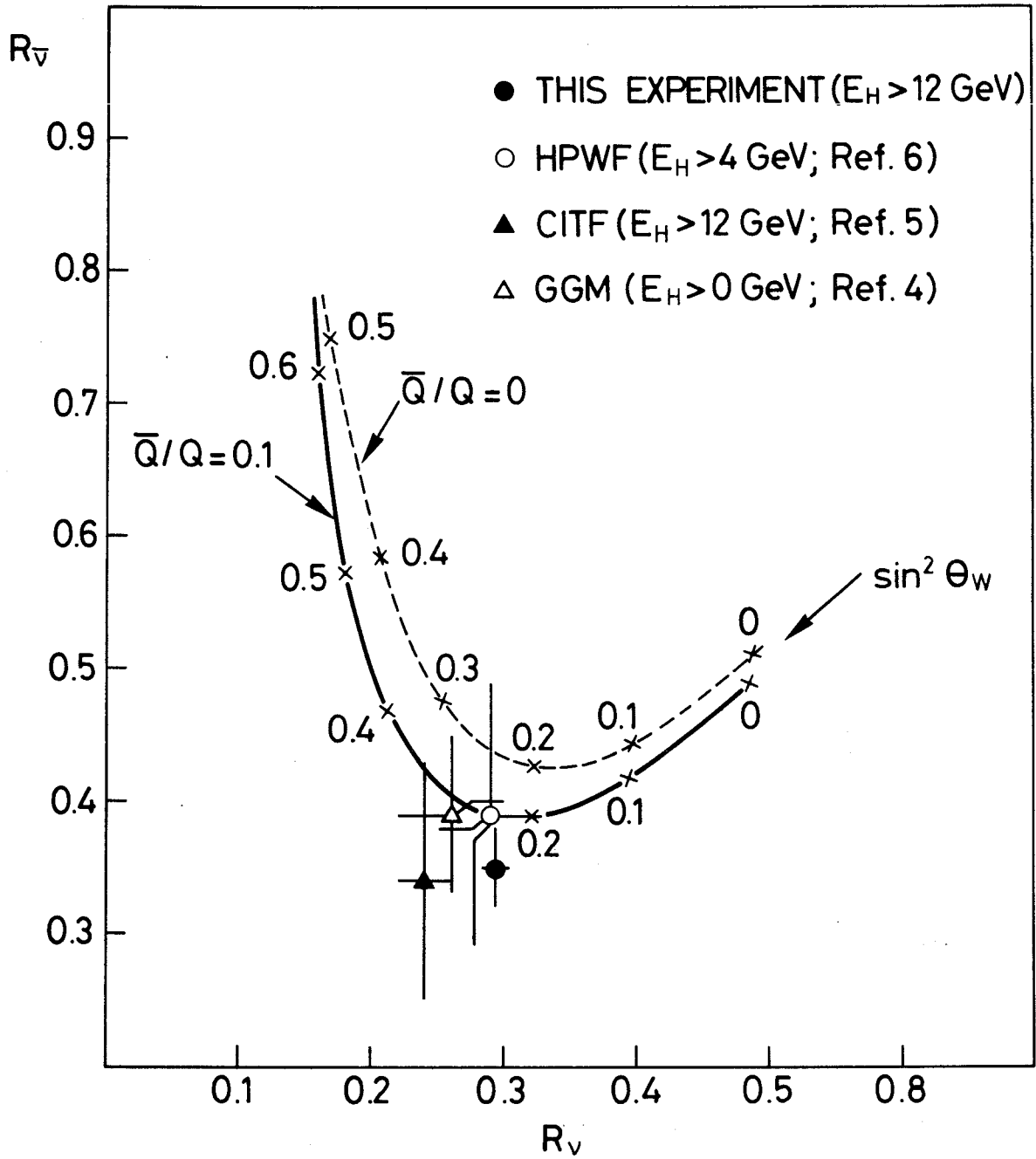


FIG. 3

1. The first part of the document discusses the importance of maintaining accurate records of all transactions.

2. It is essential to ensure that all entries are supported by appropriate documentation and receipts.

3. Regular audits should be conducted to verify the accuracy of the records and to identify any discrepancies.

4. The second part of the document outlines the procedures for handling incoming payments and deposits.

5. All payments should be recorded promptly and accurately, and the corresponding receipts should be filed.

6. The third part of the document describes the process for issuing invoices and bills to customers.

7. Invoices should be prepared clearly and accurately, and sent to customers in a timely manner.

8. The fourth part of the document discusses the methods for reconciling bank statements and accounts.

9. Regular reconciliations should be performed to ensure that the company's records match the bank's records.

10. The final part of the document provides a summary of the key points and offers recommendations for improving financial management.

11
12
13
14
15
16
17
18
19
20
21
22
23
24
25
26
27
28
29
30
31
32
33
34
35
36
37
38
39
40
41
42
43
44
45
46
47
48
49
50
51
52
53
54
55
56
57
58
59
60
61
62
63
64
65
66
67
68
69
70
71
72
73
74
75
76
77
78
79
80
81
82
83
84
85
86
87
88
89
90
91
92
93
94
95
96
97
98
99
100